



Author(s)	Chanslor, Richard M.
Title	An analysis of a current regulator for a cyclotron bending magnet.
Publisher	Monterey, California: U.S. Naval Postgraduate School
Issue Date	1963
URL	<a href="http://hdl.handle.net/10945/11604">http://hdl.handle.net/10945/11604</a>

This document was downloaded on May 22, 2015 at 07:56:43



<http://www.nps.edu/library>

Calhoun is a project of the Dudley Knox Library at NPS, furthering the precepts and goals of open government and government transparency. All information contained herein has been approved for release by the NPS Public Affairs Officer.

**Dudley Knox Library / Naval Postgraduate School  
411 Dyer Road / 1 University Circle  
Monterey, California USA 93943**



<http://www.nps.edu/>

NPS ARCHIVE  
1963  
CHANSLOR, R.

AN ANALYSIS OF A CURRENT REGULATOR  
FOR A CYCLOTRON BENDING MAGNET  
RICHARD M. CHANSLOR

LIBRARY  
U.S. NAVAL POSTGRADUATE SCHOOL  
MONTEREY, CALIFORNIA

AN ANALYSIS OF A CURRENT REGULATOR  
FOR A  
CYCLOTRON BENDING MAGNET

\* \* \* \* \*

Richard N. Chanslor

AN ANALYSIS OF A CURRENT REGULATOR  
FOR A  
CYCLOTRON BENDING MAGNET

By

Richard M. Chanslor  
//  
Lieutenant, United States Navy

Submitted in partial fulfillment of  
the requirements for the Degree of

MASTER OF SCIENCE  
IN  
ELECTRICAL ENGINEERING

United States Naval Postgraduate School  
Monterey, California

1 9 6 3

AN ANALYSIS OF A CURRENT REGULATOR  
FOR A  
CYCLOTRON BENDING MAGNET

By

Richard M. Chanslor

This work is accepted as fulfilling  
the thesis requirements for the degree of


MASTER OF SCIENCE

IN

ELECTRICAL ENGINEERING

from the

United States Naval Postgraduate School



## ABSTRACT

This paper reports the results of an analysis of a current regulating system for a cyclotron bending magnet at the 90" cyclotron, Lawrence Radiation Laboratory, Livermore, California.

The analysis was conducted in order to determine why the system did not regulate sufficiently at certain times.

The observations made, and data obtained made it possible to determine the causes of two factors which did not appear in the circuit representation used in design, thereby reducing the problem to one of correcting those two factors---namely, noise from the generator, and the operation of the D. C. amplification stage,  $K_2$ .

## TABLE OF CONTENTS

Section	Title	Page
1.	Introduction	1
2.	Theory	4
3.	Preliminary Analysis	10
4.	Experimental Analysis	20
5.	Conclusions	33
6.	Bibliography	35
	Appendix I - Generator Frequency Responses	36
	Appendix II - Magnet Frequency Responses	40

## LIST OF ILLUSTRATIONS

Figure	Title	Page
1-1	Regulating System Diagram	2
2-1	Nonlinear System Block Diagram	5
2-2	Stability Investigation Using a Describing Function	6
2-3	Graphical Determination of a Describing Function	7
2-4	Graphical Determination of a Describing Function	8
3-1	Regulating System Block Diagram	11
3-2	Determination of Limiting Time Constants for the Generator	12
3-3	Uncompensated System Root Locus	14
3-4	Compensated System Root Locus Using $G_F$	16
3-5	Compensated System Root Locus Using $G_{F^*}$	17
3-6	Compensated System Bode Plots	19
4-1	Test Equipment Diagram	22
4-2	Generator Frequency Response	24
4-3	Generator Frequency Response with Magnet Connected	25
4-4	Magnet Frequency Responses	27
4-5	Average Magnet Frequency Response	28
4-6	Magnet Approximation	29
4-7	Compensated System Root Locus	30
4-8	Bode Diagram for Compensated System	31

## 1. Introduction

The 90" Cyclotron at the Lawrence Radiation Laboratory, Livermore, California employs two bending magnets which are used in certain experiments to direct a beam of particles onto a given target.

Since the target distances are great and the size of the targets small, it is necessary to apply an extremely well regulated current supply to the bending magnets in order to keep the beams on target.

For this purpose, two identical regulating systems are used with two motor-generator sets to supply the current. The generators are rated at 20 KW, 160 amps at 125 volts d.c. The systems were designed to provide stable operation with better than 0.1% regulated current over the range from 15 amps to 100 amps. A diagram of the regulating system is Fig. 1-1. An analysis of this system was to be carried out, in an attempt to determine why it was not performing in a fully acceptable way.

The regulator's operation was not completely satisfactory and it was suggested that the reason might be nonlinear operation not accounted for in the original design. The original design procedure involved frequency response methods which presented no investigation of the possibility that nonlinear effects might be important over the range of operation.

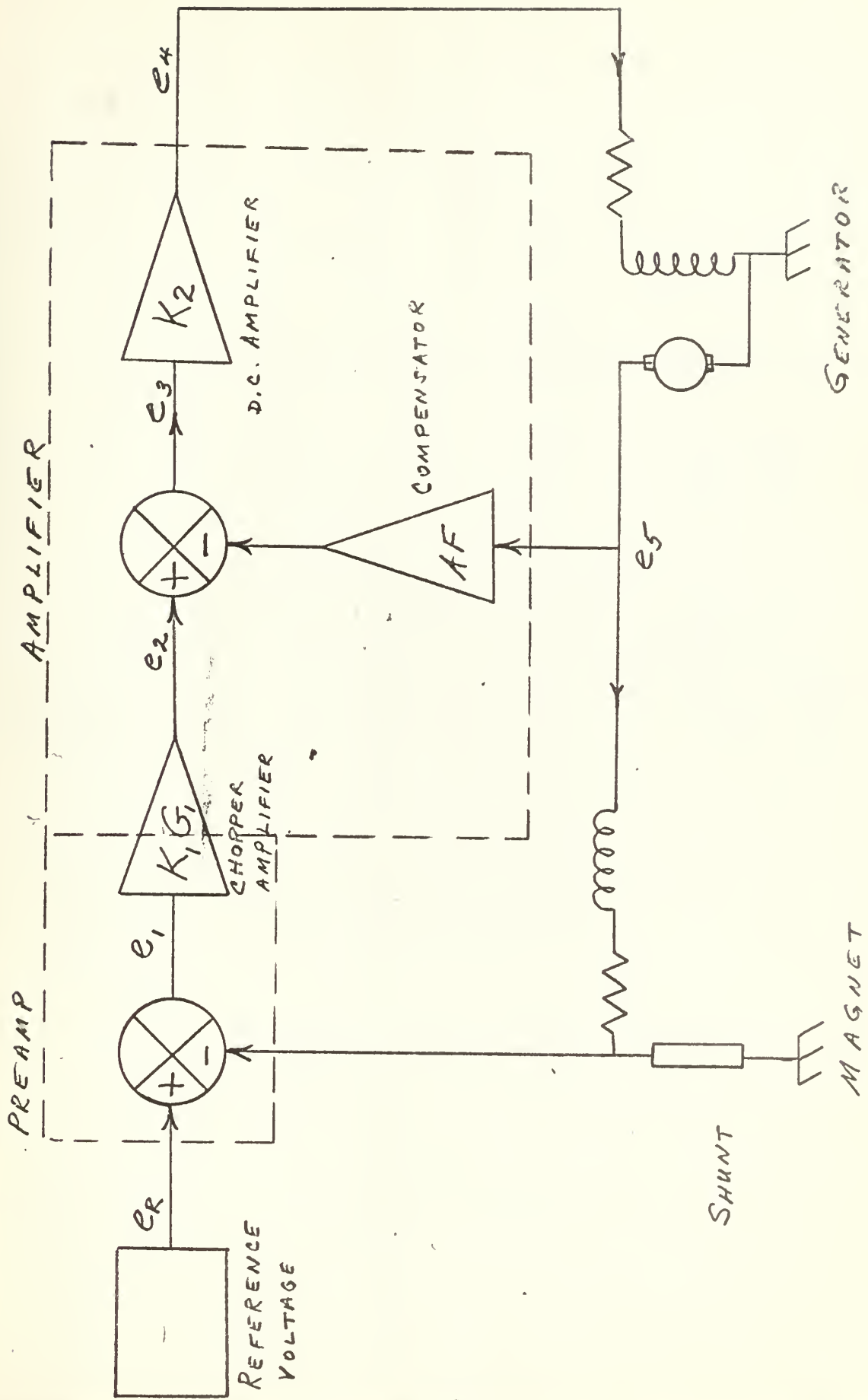


FIGURE I-1. REGULATING SYSTEM DIAGRAM

No systematic record of deficiencies or failures was available, but some comments from cyclotron operators and technicians indicated that sometimes the beam strayed off target and oscillated, after large changes in magnet current operating level.

The plan of attack for the problem was:

1. To make a preliminary analysis of the system, using the original design data.
2. To observe the system in actual operation and take experimental measurements as necessary, including investigation of nonlinearity to make certain that a suitable analytical model was established.
3. To analyze the system on the basis of that model, and make recommendations for improvement.

Since the magnet was the chief candidate for the suspected nonlinearity, the greatest part of the problem became the analysis of the magnet in order to determine the extent to which it was nonlinear, and how it was effecting the operation. The next section explains the method of attack employed, and discusses the theory behind it.

## 2. Theory

In the study of linear systems, the use of the block diagram and transfer functions to represent the system components is extremely useful. When one of the components is a nonlinear element, the block diagram may still be used, realizing that the transfer function concept is no longer valid for the nonlinear block.

Since such a nonlinear block was suspected to exist in the system under study, the attack used in the problem included nonlinear techniques which would provide a suitable representation for the nonlinearity, which could be used in the block diagram.

One solution is to use the describing function, or approximate transfer function which may be defined as follows. (2)

Assuming that the input to the nonlinear block is of the form:

$$\text{Input} = A \sin \omega t$$

then the Fourier series fundamental of the output is

$$F(A, \omega) \sin [\omega t + \phi(A, \omega)] .$$

And the describing function is defined as:

$$G_D(A, \omega) = \left| \frac{F(A, \omega)}{A} \right| \angle \phi(A, \omega)$$

If the approximation is close enough,  $G_D(A, \omega)$  may be used in the block diagram.

A method of evaluating the describing function involves taking frequency responses of the nonlinear

block, and using an overlay technique with the Nichols chart, to plot a curve of  $\frac{1}{G_D}$ .

If, in the system under study, the magnet were nonlinear, and if it could be represented by a describing function,  $G_D$ , then the system block diagram could be reduced to that shown below, where  $G_D$  represents the magnet describing function and  $G_1$ , the remaining, linear part of the system.

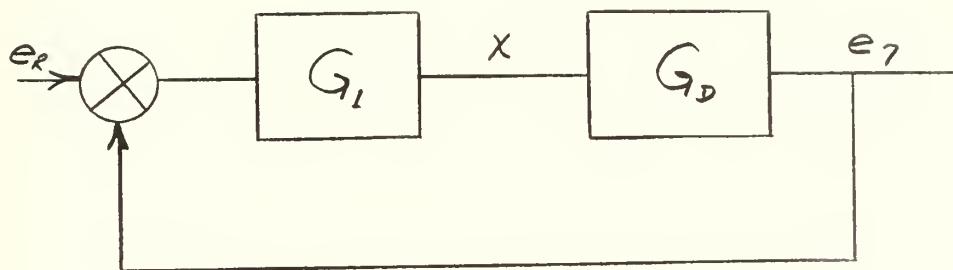


Fig. 2-1 Nonlinear System Block Diagram

$$\frac{e_1}{e_R} = \frac{G_1 G_D}{1 + G_1 G_D}$$

At the limit of stability:

$$G_1 G_D = -1$$

or:

$$G_1 = -\frac{1}{G_D}$$

So that for the amplitude sensitive nonlinearity, where  $-\frac{1}{G_D}$  is a single curve, stability may be examined by checking for intersections of curves of  $G_1$  and  $-\frac{1}{G_D}$  on the Nichols plot. These might appear as sketched on the next page.

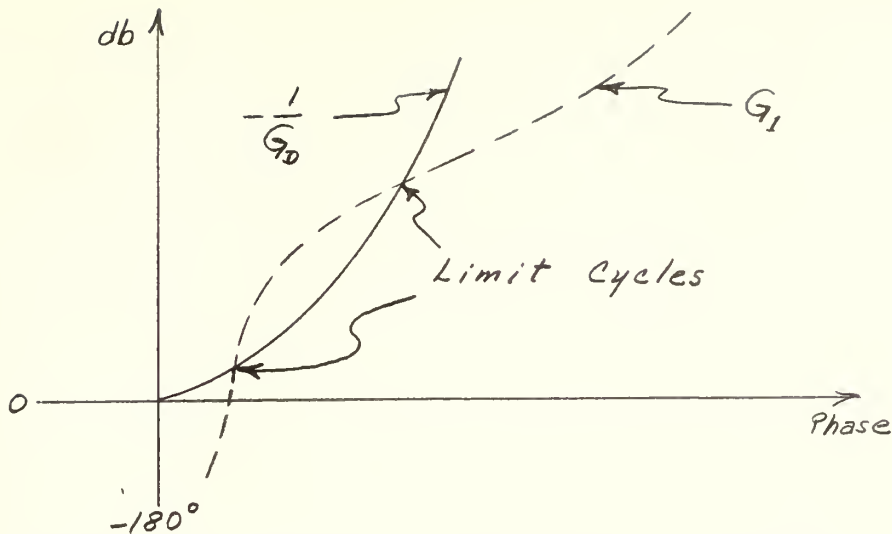


Fig. 2-2 Stability Investigation, Using a Describing Function

Each position along  $-\frac{1}{G_D}$  represents magnitude and phase for a particular value of input magnitude to the nonlinear block.

A procedure for determining the  $-\frac{1}{G_D}$  curve experimentally is as follows:

1. Measure a frequency response for  $G_1$ ,  $G_D$  at a certain amplitude of input,  $x_1$ , to the non-linearity, and make a smooth Bode plot.
2. Plot this curve on a Nichols chart, noting values of  $\omega$  (frequency) and  $x$ .
3. Repeat for various values of  $x$ .

When  $G_1 G_D$  is plotted on the Nichols chart, the origin of the Nichols plot represents the point  $1 / \underline{180^\circ}$ , and if  $G_1 G_D$  passes through this point then,

$$G_1 G_D = -1 \quad \text{or} \quad G_1 = -\frac{1}{G_D},$$

indicating the limit of stability. This point might be called the critical point.

If the  $G_D$  block is nonlinear, the curve  $G_1 G_D$  will move with changes in  $x$ . But since  $G_D$  is the only

part which changes with  $x$ , then the movement of the curve must be caused by  $G_D$ .

If instead of looking at the locus of  $G_1 G_D$  curves, the locus of the critical point relative to the succession of  $G_1 G_D$  curves is observed, this locus of critical points will be the  $-\frac{1}{G_D}$  curve.

For example:

Suppose that the sketch below shows a Nichols plot of  $G_1 G_D$  (solid curve) for  $x = x_1$ , and a point of  $-\frac{1}{G_D}$  is at the origin:

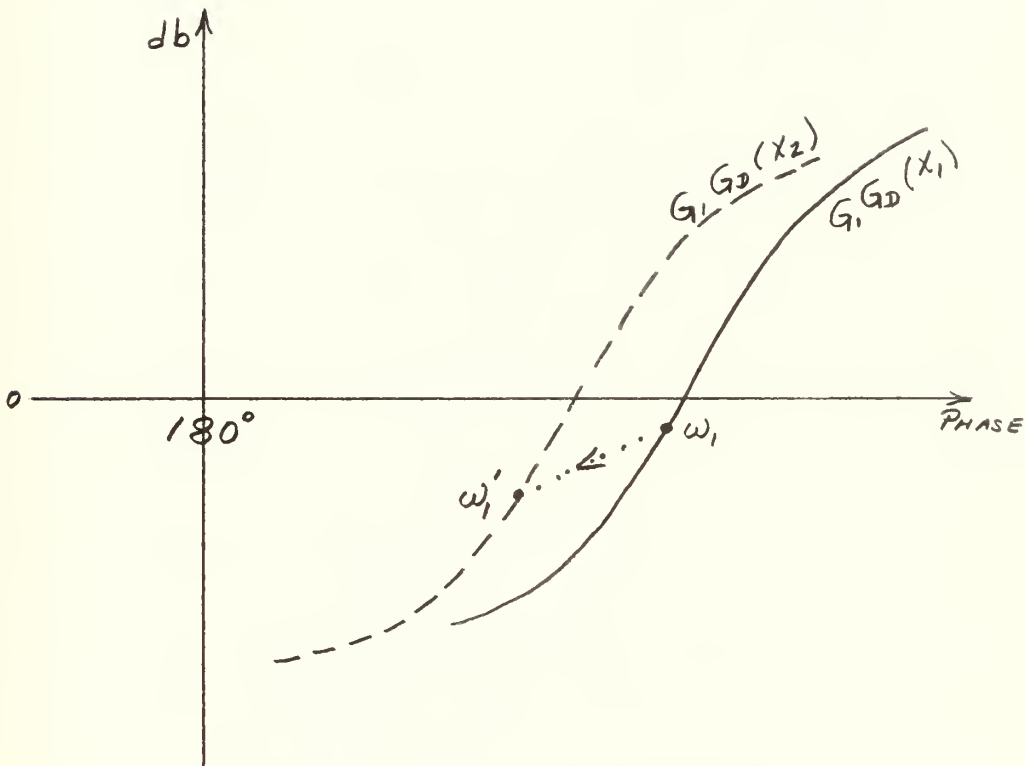


Fig. 2-3 Graphical Determination at a Describing Function

The dashed curve might represent  $G_1 G_D$  for  $x = x_2$ . Place an overlay sheet over the Nichols plot and trace the 0 db and  $180^\circ$  axes (intersecting at the critical point, point 0) and the  $x_1$  curve (including frequency

locations). Then adjust the overlay until this traced curve is matched with the  $x_2$  curve. Now mark the origin of the Nichols plot on the overlay again. This new point on the overlay sheet represents a second point on the critical point locus which is the  $-\frac{1}{G_D}$  curve, as sketched below.

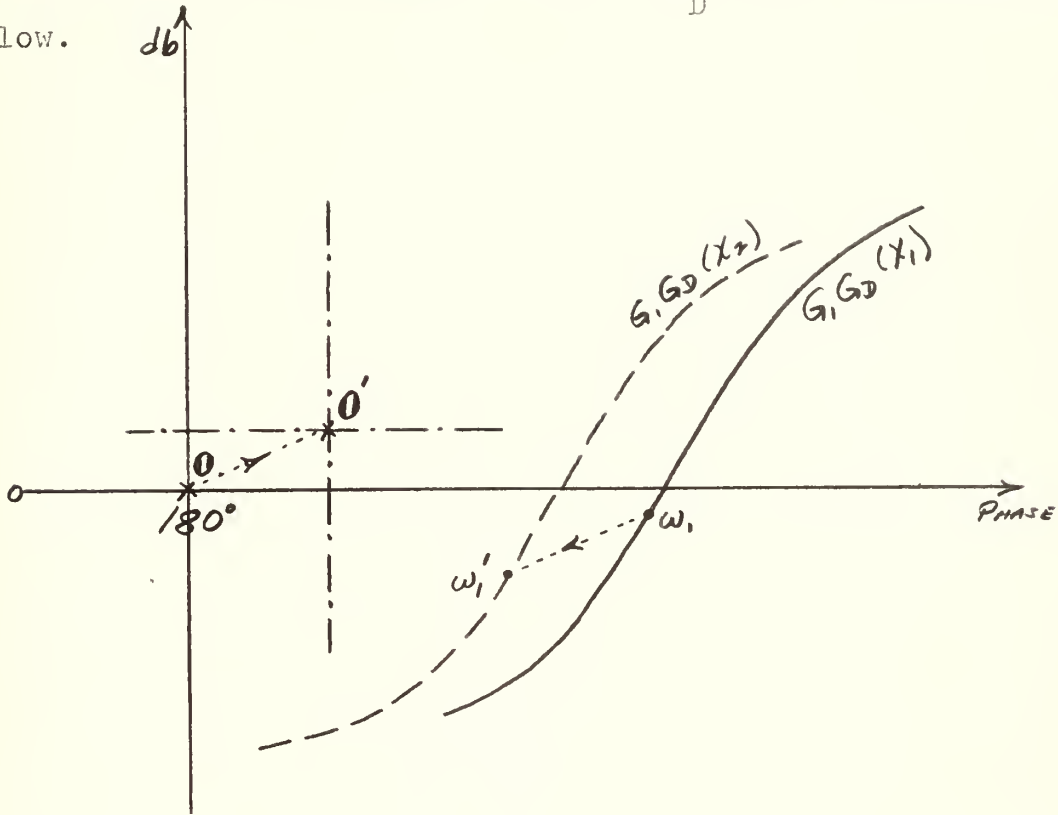


Fig. 2-4 Graphical Determination of a Describing Function

Continue for other values of  $x$  until the entire  $-\frac{1}{G_D}$  curve is obtained.

So: 4. For each succeeding value of  $x$ , use the overlay technique to plot a corresponding point on the  $-\frac{1}{G_D}$  curve.

This describing function theory provided the basis for the experimental work done in section four, which was directed toward evaluating a describing function to represent the magnet in the system block diagram.

Chapter four of reference two, Analysis and Design of Nonlinear Feedback Control Systems by Thaler and Iastel presents a detailed discussion of the describing function and its application.

### 3. Preliminary Analysis

The preliminary analysis was carried out using the results of the original design work, with some modifications as explained below.

The block diagram shown in Fig. 3-1 illustrates the regulating system along with transfer functions determined from the original design work.

Note that the generator and magnet each have two transfer functions indicated, which are an attempt to establish two limiting values for the transfer function of the system. Their original design transfer functions were presented as:

$$K_3 G_3 = K_G \left[ \frac{1}{(j\omega T_f + 1)^n} \right] ; (n = .9)$$

for the generator, and:

$$K_4 G_4 = K_m \left[ \frac{1}{(j\omega T_m + 1)^n} \right] ; (n = .5)$$

for the magnet.

These exponents,  $n$ , were introduced in an attempt to account for the fact that the experimental frequency response curves used to obtain these transfer functions fell off toward asymptotes with slopes other than 20 db/decade.

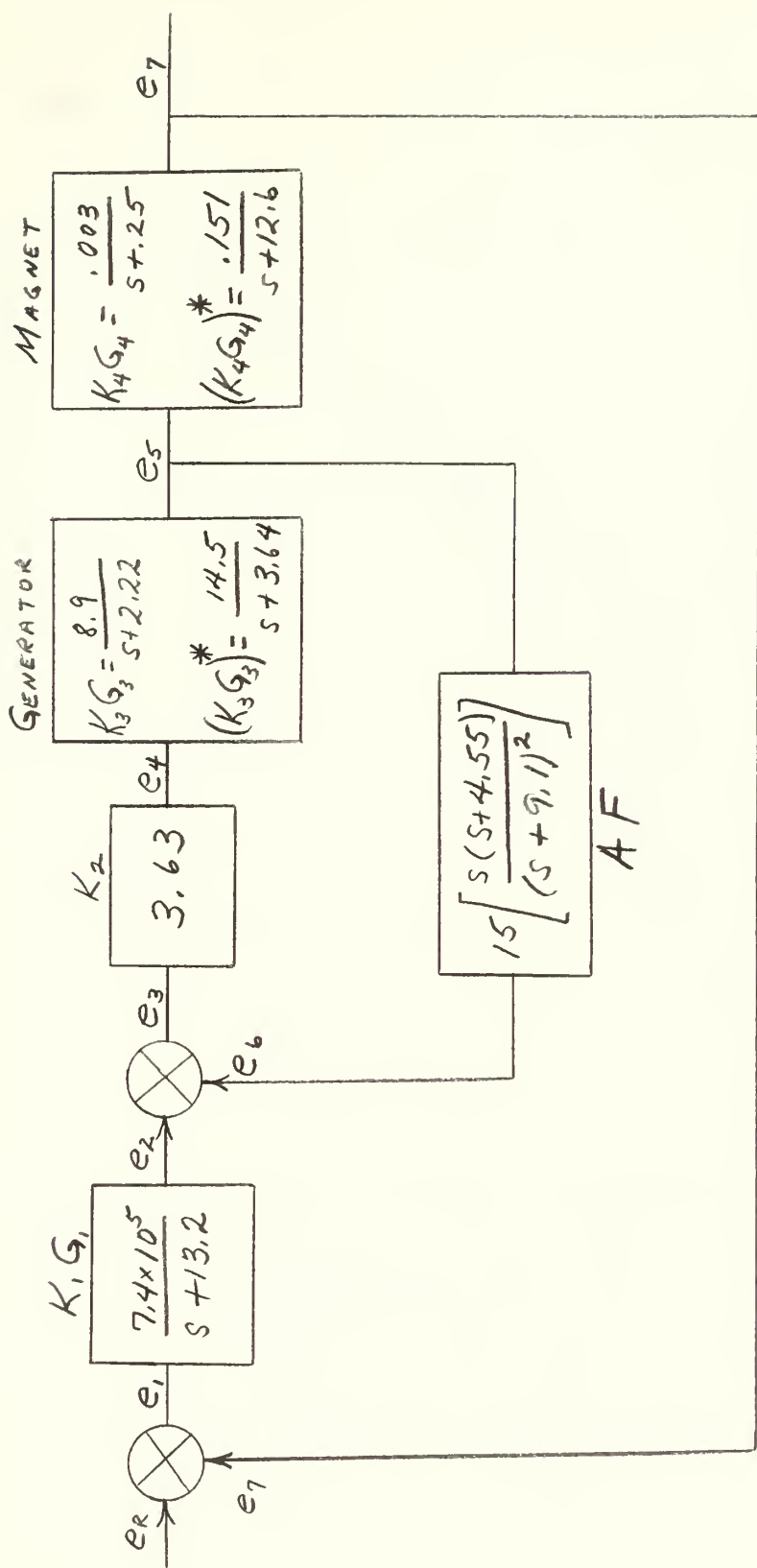


FIG. 3-1 REGULATING SYSTEM BLOCK DIAGRAM

Fig. 3-2 gives a copy of the original magnitude plot for the generator. Instead of accepting the transfer functions

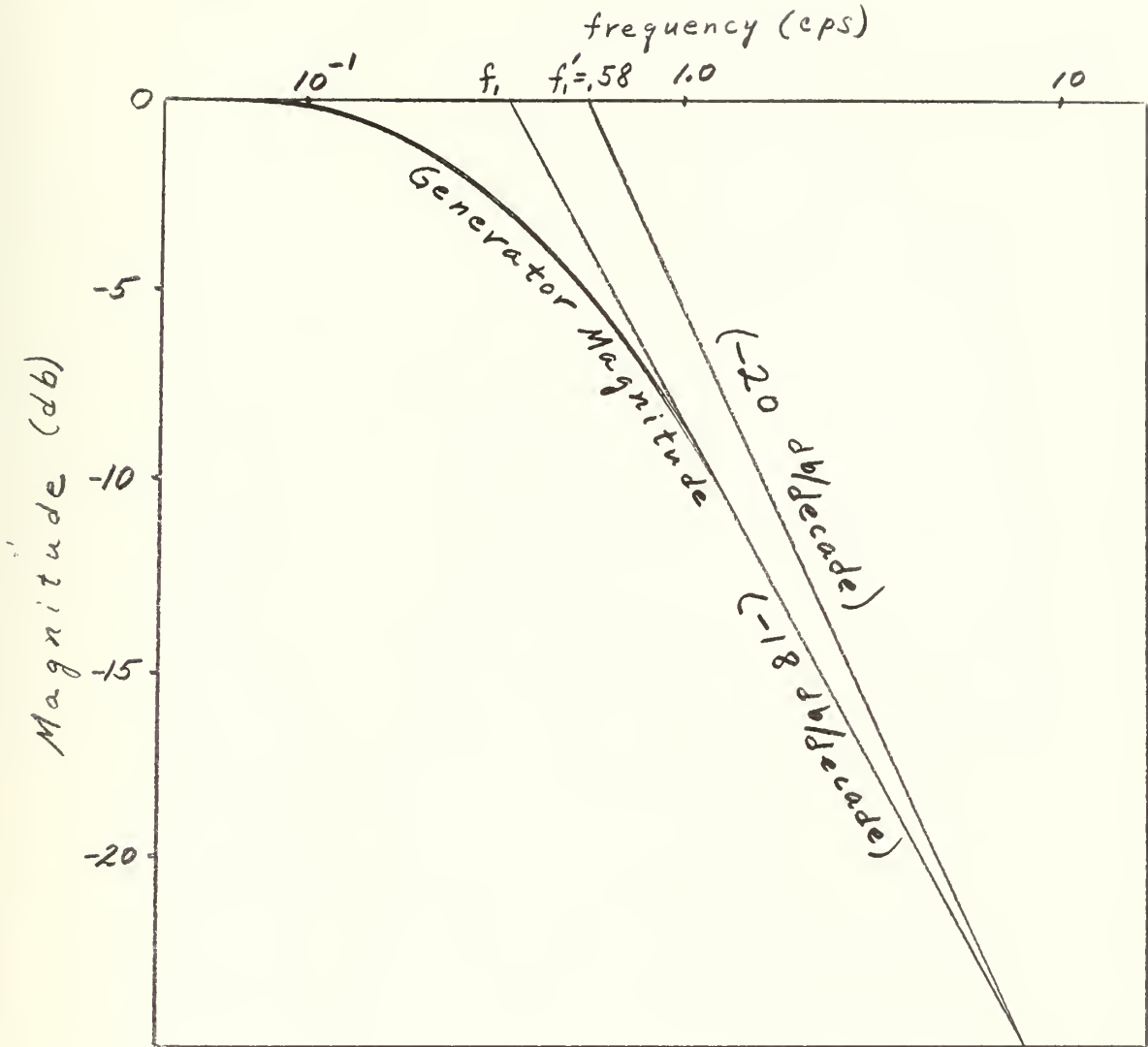


Fig. 3-2 Determination of Limiting Time Constants for the Generator

with the exponents, two limiting values for  $K_3 G_3$  were obtained which, it was hoped, would bracket the actual condition. One of these was gotten just by setting  $n=1$  and accepting the original value of  $T_f=(0.45)$ . Then

$$K_3 G_3 = \frac{4}{8(0.45) + 1} . \text{ For the other limiting value,}$$

the magnitude plot was forced to approach a 20 db/decade asymptote as shown in Fig. 3-2, defining the point  $f_1' = 0.58$ , from which:

$$\omega T_f' = 2\pi f_1' T_f' = 1$$

$$T_f' = \frac{1}{2\pi f_1'} = \frac{1}{2\pi(0.58)} = 0.275$$

so that:  $(K_3 G_3)^* = \frac{4}{s(.275) + 1}$

By the same technique, limiting values of  $K_4 G_4$  for the magnet were obtained as:

$$K_4 G_4 = \frac{.012}{s(4.0) + 1} \quad \text{and} \quad (K_4 G_4)^* = \frac{.012}{s(.0795) + 1}$$

Looking at the block diagram of Fig. 3-1 the resulting pair of transfer functions for the uncompensated system became:

$$G_o = (K_1 G_1)(K_2)(K_3 G_3)(K_4 G_4)$$

$$= \frac{7.17 \times 10^4}{(s+13.2)(s+2.22)(s+.25)}$$

$$G_o^* = (K_1 G_1)(K_2)(K_3 G_3)^*(K_4 G_4)^*$$

$$= \frac{5.88 \times 10^6}{(s+13.2)(s+3.64)(s+12.6)}$$

The root locus plots for these are shown in Fig. 3-3 and either plot indicates that the system is very unstable, as expected.

Introducing the feedback compensation loop, AF, the transfer functions for the compensated system become:

$$G_F = \frac{7.18 \times 10^4 (s+9.1)^2}{(s+13.2)(s+499.7)(s+.08)(s+4.58)(s+.25)}$$

and

$$G_F^* = \frac{(5.89 \times 10^6) (s+9.1)^2}{(s+13.2)(s+806.7)(s+4.56)(s+.085)(s+12.6)}$$

The regulation desired was 0.1%. The system functions

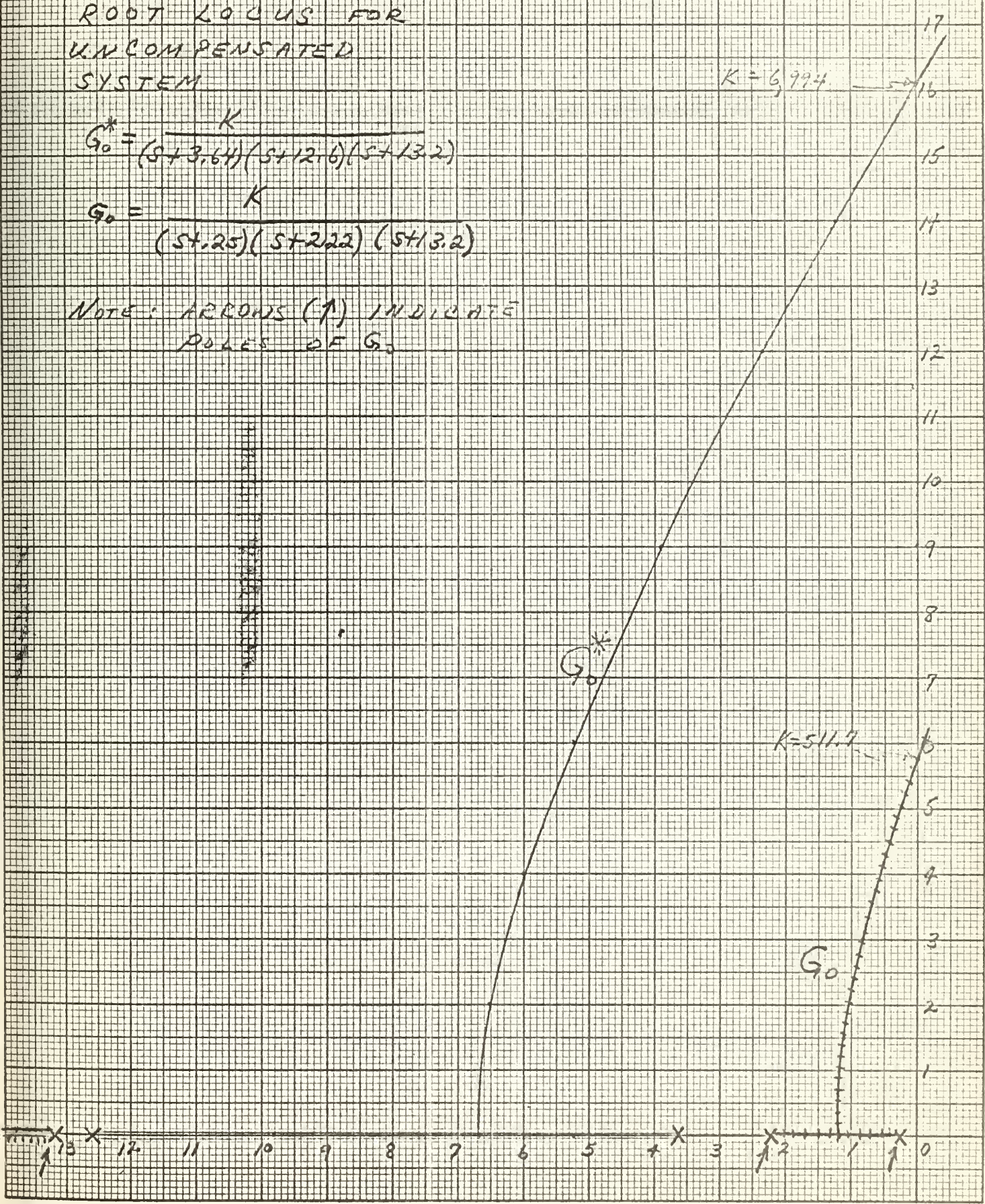
# FIG. 3-3

ROOT LOCUS FOR  
UNCOMPENSATED  
SYSTEM

$$G_o^* = \frac{K}{(s+3.64)(s+12.6)(s+13.2)}$$

$$G_o = \frac{K}{(s+2.25)(s+2.22)(s+13.2)}$$

NOTE: ARROWS (↑) INDICATE  
POLES OF  $G_o$



become:  $\frac{G_F}{1+G_F}$ , and  $\frac{G_{F^*}}{1+G_{F^*}}$ , so that for the un-starred quantities, application of the final value theorem leads to the fact that  $e_7$  (output) =  $\frac{e_R}{1.00010}$ .

$$\text{For } \frac{G_{F^*}}{1+G_{F^*}}, e_7 = \frac{e_R}{1.00008}$$

Both pass the .1% regulation requirement by a factor of about ten.

The root loci for  $G_F$  and  $G_{F^*}$  are shown in Fig. 3-4 and 3-5. The  $G_F$  locus shows the system still unstable for the gain used. The  $G_{F^*}$  locus indicates a stable system, but still very lightly damped. However, if the gain were reduced by a factor of ten, the .1% regulation specification would still be met, and the system would be well enough damped for satisfactory operation.

Thus if it were acceptable to assume that the actual operation was bracketed by the  $G_F$  and  $G_{F^*}$  conditions, there would arise some doubt as to whether the operation would be satisfactory, depending upon whether  $G_F$  or  $G_{F^*}$  was more nearly correct.

Bode diagrams were also plotted for  $G_F$  and  $G_{F^*}$  since the plot from the original design was available for comparison.

In frequency response form:

$$G_F = \frac{9.82 \times 10^3 (j \frac{f}{1.45} + 1)^2}{(j \frac{f}{0.01275} + 1)(j \frac{f}{0.0398} + 1)(j \frac{f}{.730} + 1)(j \frac{f}{2.10} + 1)(j \frac{f}{79.5} + 1)}$$

FIG 3-4

$$S_f = \frac{7.175 \times 10^4 (654.9)^2}{(5.13.2)(5 + 499.7) (54.08) (854.5) (54.25)}$$

$$K = 5 \times 10^3$$

5  
499.7

13 12 11 10 9 8 7 6 5 4 3 2 1

14 13 12 11 10 9 8 7 6 5 4 3 2 1

14 13 12 11 10 9 8 7 6 5 4 3 2 1

14 13 12 11 10 9 8 7 6 5 4 3 2 1

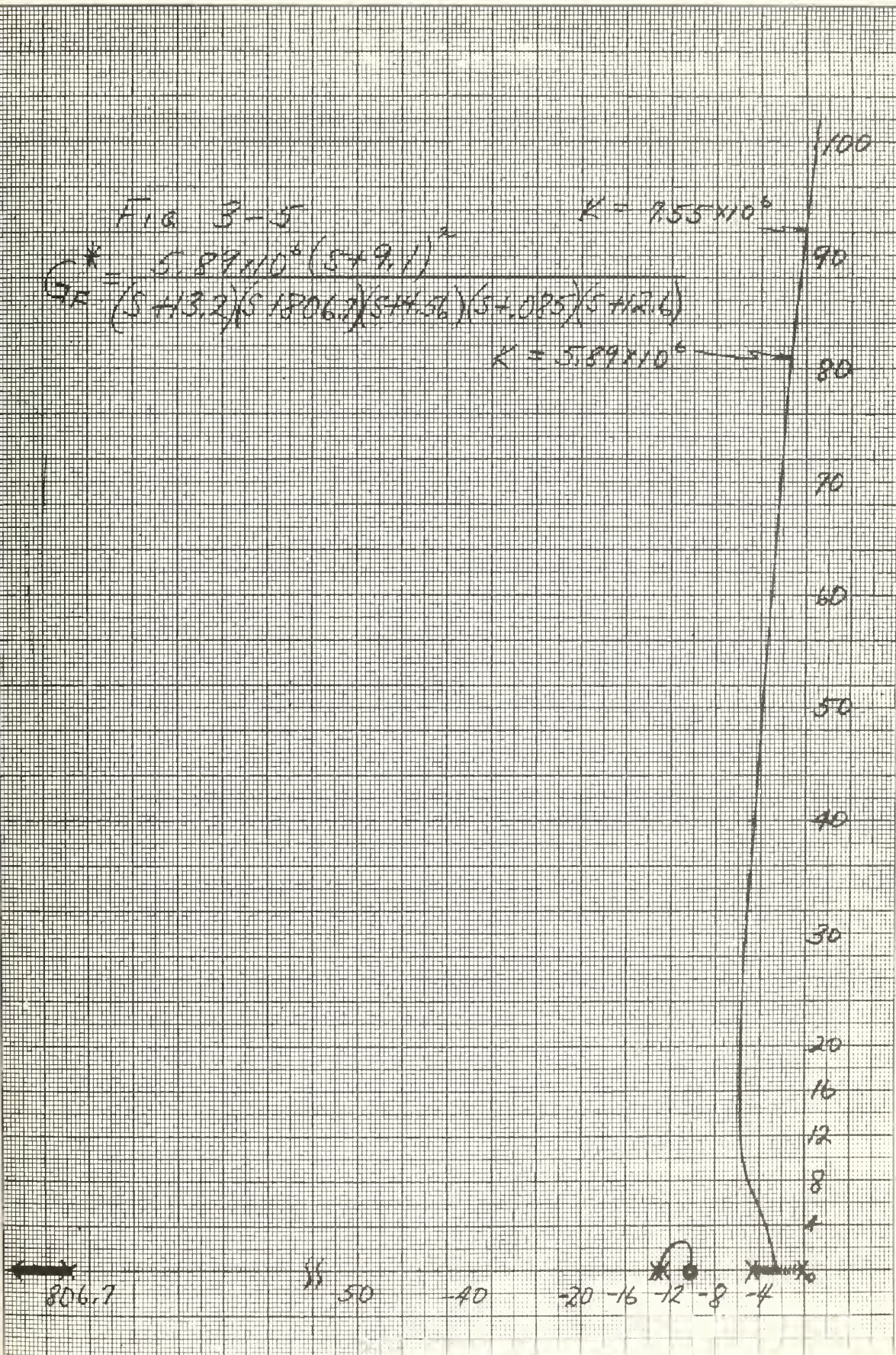
14 13 12 11 10 9 8 7 6 5 4 3 2 1

FIG 3-5

$$K = 7.55 \times 10^6$$

$$K = \frac{5.89 \times 10^6 (5 + 9.1)^2}{(5 + 13.2)(5 + 18.067)(5 + 11.56)(5 + 1.085)(5 + 12.6)}$$

$$K = 5.89 \times 10^6$$



$$\text{and: } G_F^* = \frac{9.36 \times 10^3 (j^{+1/1.45} + 1)^2}{(j \frac{f}{0.136} + 1)(j \frac{f}{725} + 1)(j \frac{f}{2} + 1)(j \frac{f}{2.1} + 1)(j \frac{f}{128.5} + 1)}$$

These were written in terms of  $f$ , frequency, instead of the usual  $\omega$ , for comparison with the original frequency response plot.

The magnitude plots for  $G_F$  and  $G_F^*$  compared with that presented with the original design,  $G(s)$ , appear in Fig. 3-6.

The  $G_F$  and  $G_F^*$  plots do bracket the  $G(s)$  curve, but for  $G(s)$ , a phase margin of  $+30^\circ$  was indicated, while those predicted by  $G_F$  and  $G_F^*$  were  $-6.7^\circ$  and  $+2^\circ$  respectively. These results were consistent with the root locus results, but conflicted with the design report, casting some doubt as to whether the system was adequately compensated.

Plans for the remainder of the analysis were to observe and assess the actual operation of the regulating system, and to investigate the nonlinearity of the magnet circuit so that recommendations for improvement could be made.



#### 4. Experimental Analysis

Closed loop operation of the system was observed, and over most of the operating range of magnet currents, the system appeared to be satisfactory, stable, and well regulated. However, when adjusted for operation at low magnet current, about 20 amps, it was possible to produce an unsatisfactory condition with an oscillatory output and insufficient regulation by changing the reference level to give a magnet current of about 100 amps.

In the existing system, two filters appear which were added for additional noise suppression, after the original design was completed.

One of these is a parallel tee filter which appears in the minor feedback (compensator) loop, in the block labeled AF in Fig. 1-1. The filter is located at the input to the pentode labeled V-5 of this amplifier. Analysis of this parallel tee, showed that its effect is negligible in the operating range, and can be neglected in the system block diagram.

The second filter mentioned is a lead-lag filter followed by a parallel tee. This one is located between the chopper demodulator and the 12AT7 tube, which puts it in the forward path, right after  $V_1G_1$  in Fig. 1-1.

A frequency response for this filter was recorded and the results indicated that the phase shift was negligible over the operating range, but that the filter produced an attenuation of about ten db over the range.

This attenuation greatly decreases the error in accuracy over the steady state accuracy requirement, as calculated in section three.

In order to investigate the performance of the generator and especially the magnet, by frequency response techniques, the testing and measuring equipment was set up as shown schematically in Fig. 4-1.

The most convenient point for introducing the test signals was at the input to  $K_2$ , the D.C. amplifier. Since this point happened to be at a potential of about -150 volts during operation, the battery and potentiometer,  $P_1$ , were introduced to eliminate shock hazard at the signal generator. The signal at the output terminals of the generator was extremely noisy - so much so that the noise sometimes saturated the amplifier of the recorder, giving inaccurate readings. The R-C filter shown in the diagram was introduced to eliminate this problem.

The signal  $e_7$ , from the magnet shunt, was of such a small magnitude, that the additional D.C. amplifier,  $K_R$ , was introduced to make  $e_7$  readable at the recorder. In addition, with the large amplification required before the recorder, it was necessary to remove the small amount of D.C. bias at the magnet shunt, by means of a small battery and potentiometer  $P_2$ .

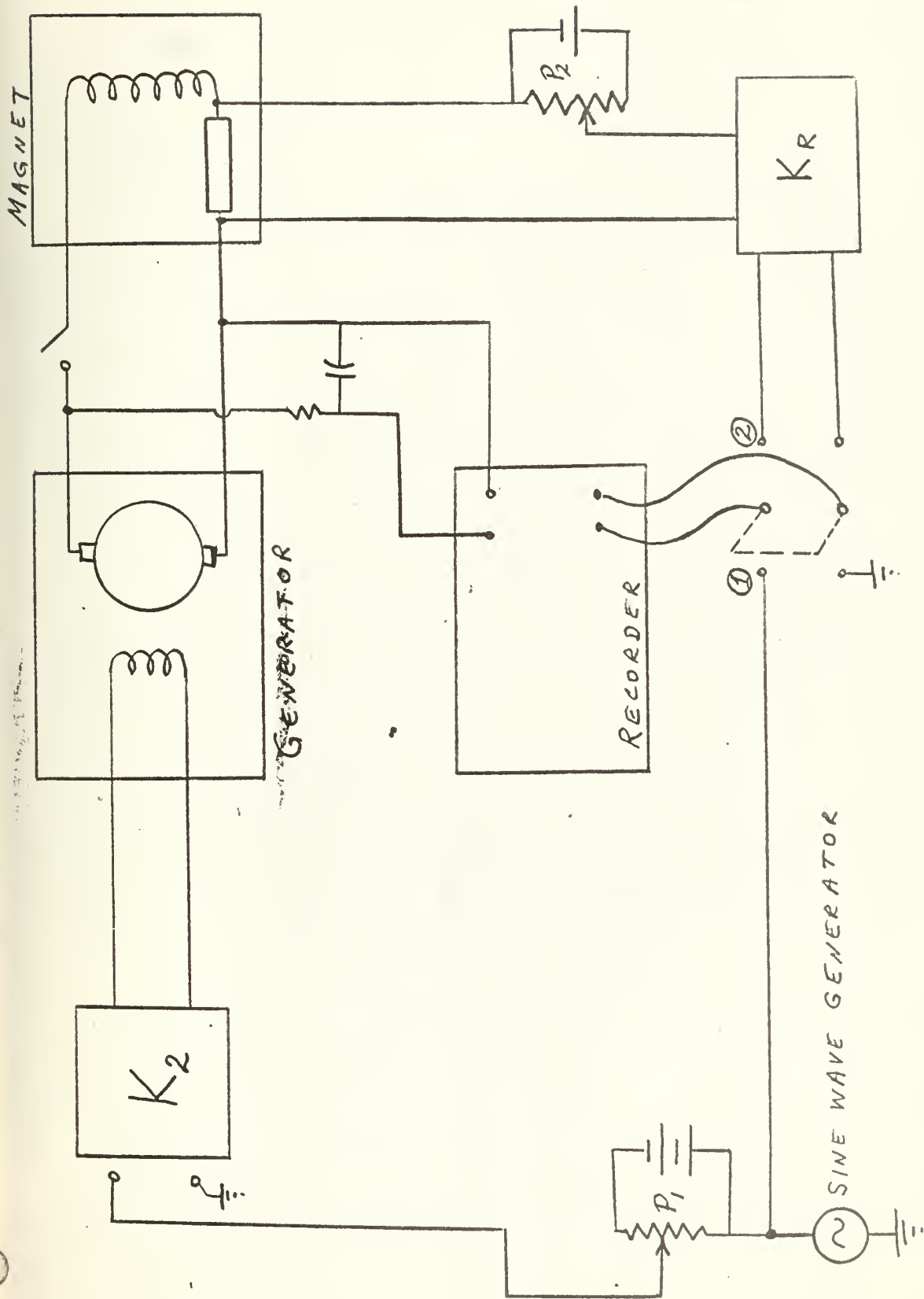


FIG. 4-1 TEST EQUIPMENT DIAGRAM

Frequency responses for the generator were taken with the magnet disconnected, and also with it connected, as in normal operation. For both conditions, responses were taken for values of input, and for magnet operating levels over the range in which the regulator was used. The generator frequency responses were essentially the same over the entire operating range. The response for the unloaded generator is shown in Fig. 4-2. Fig. 4-3 shows that the effect of connecting the magnet is just to reduce the generator voltage gain by about six db, leaving the form of the response very nearly the same as at no load. Responses for some other conditions are shown in Appendix J for comparison.

Fitting asymptotes to the loaded generator response, it is seen that the generator may be accurately described by the transfer function:

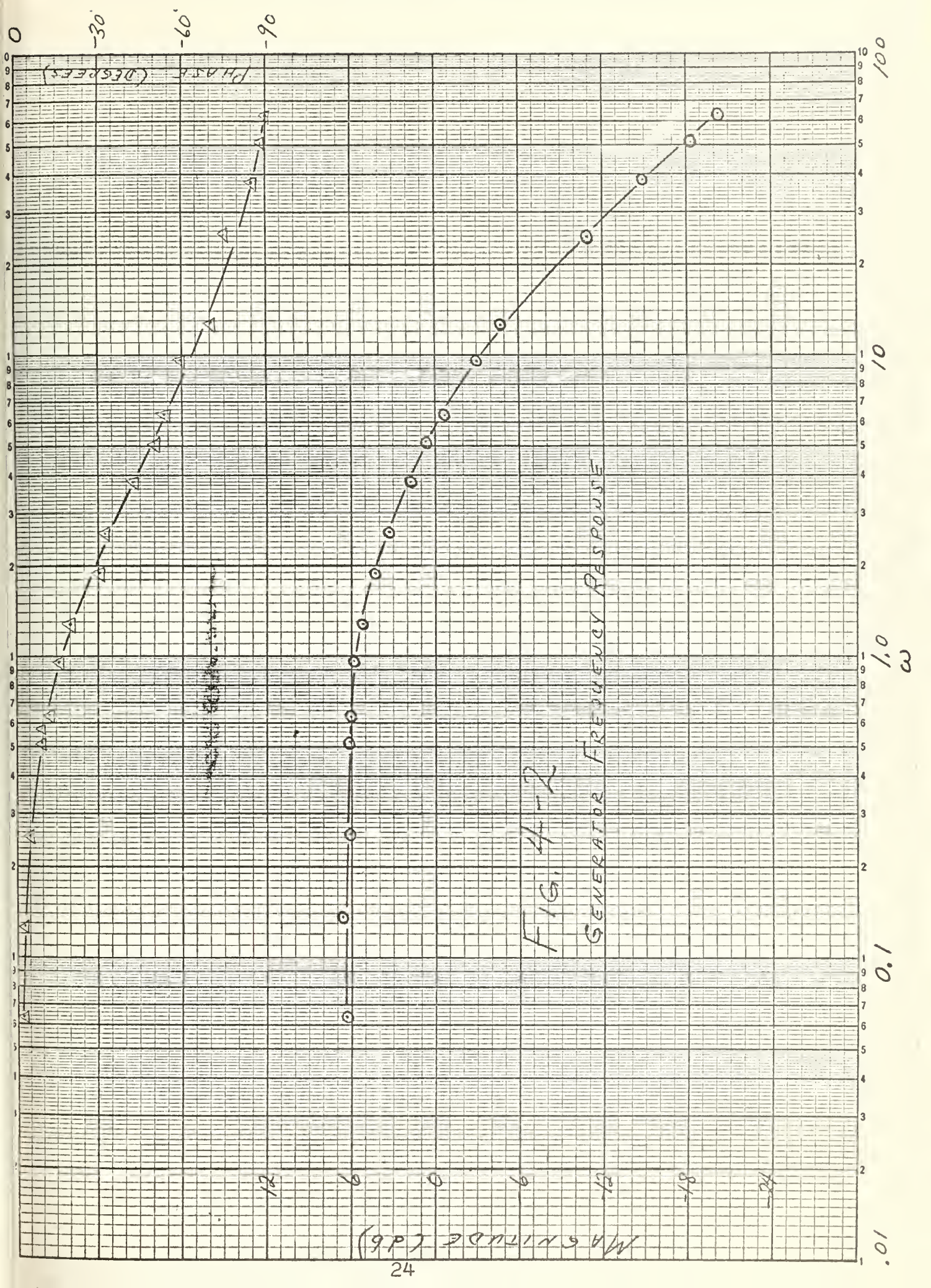
$$G_g = \frac{1.1}{(s/3.75+1)} = \frac{4.12}{s+3.75}$$

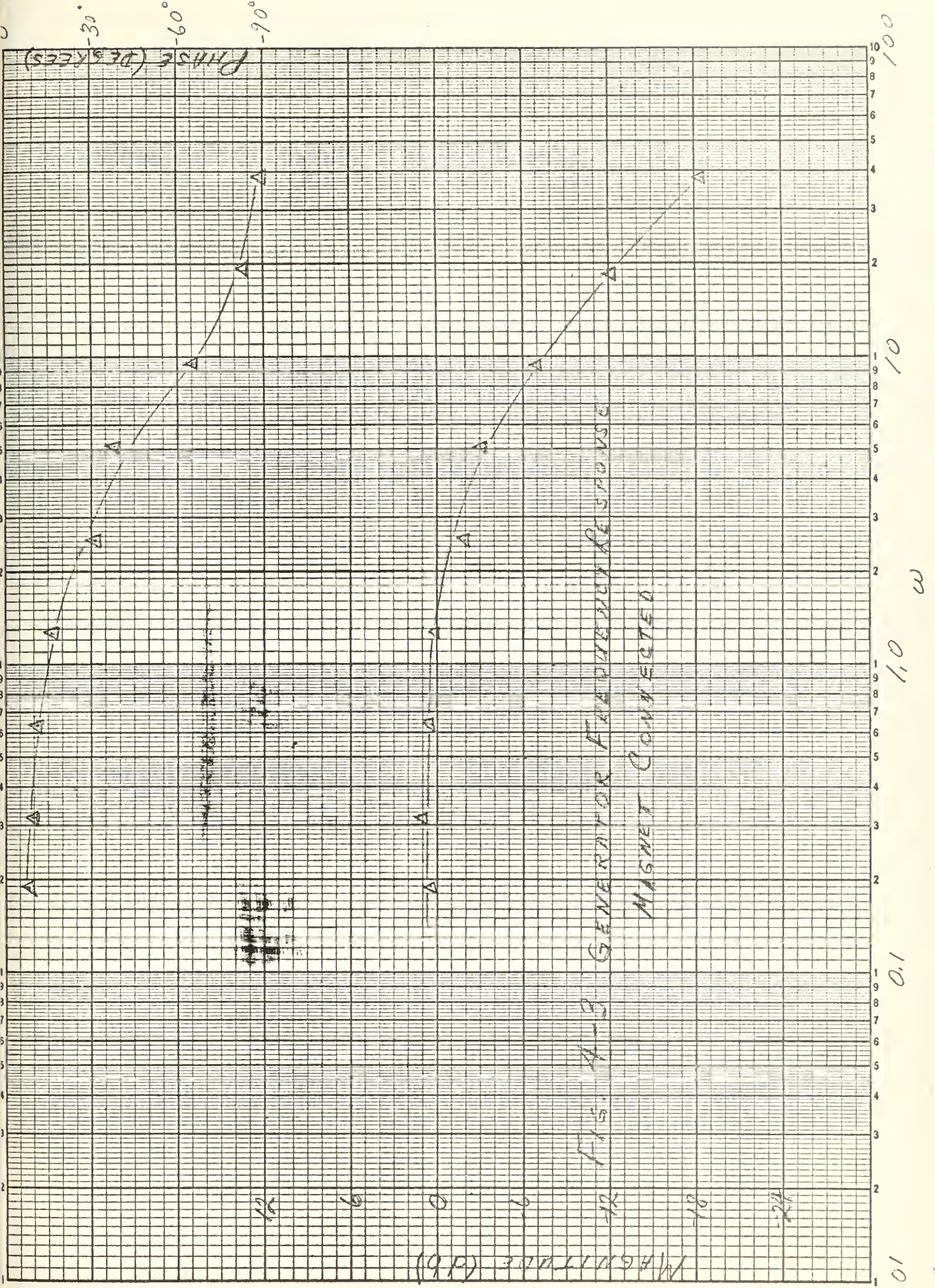
The original transfer function was:

$$K_3 G_3 = \frac{4}{(s/2.22+1)^2} = \frac{8.32}{(s+2.22)^2}$$

For the magnet frequency responses, for reasons explained in section 2, it was desired to take data over the range of possible magnet currents and at each of these values of magnet current, to record the response for several different amplitudes of input sine wave.

With the switch in position one in Fig. 4-1, the sine





wave generator was adjusted until the desired output at the D.C. generator terminals (and thus the desired input at the magnet) was observed on the recorder. Then with the switch in position 2, magnet input and output were recorded.

Some of the many magnet responses plotted are contained in Appendix II. From these frequency response curves, no consistent variation could be observed which would allow the determination of a describing function by the methods of section two. A composite plot of magnet responses is in Fig. 4-4. By comparison of the results, it was concluded that within experimental accuracy, the magnet frequency response could be considered not to be amplitude sensitive. Therefore, an average frequency response, Fig. 4-5, was obtained which could be used to represent the magnet for analysis. By fitting asymptotes as shown in Fig. 4-6, a transfer function may be written to approximate the magnet as:

$$G_m = \frac{.0105 (S/2.7+1)(S/30+1)}{(S/.96+1)(S/10.7+1)}$$

Using these new transfer functions the compensated system root locus is Fig. 4-7. The corresponding Bode diagram is Fig. 4-8. Both of these plots indicate that the system should be very stable, and for steady state condition, accounting for the attenuation due to the filter following  $F_1G_1$ :

$$e_7 = \frac{e_R}{1.001}$$

which is right at the steady state requirement. However,

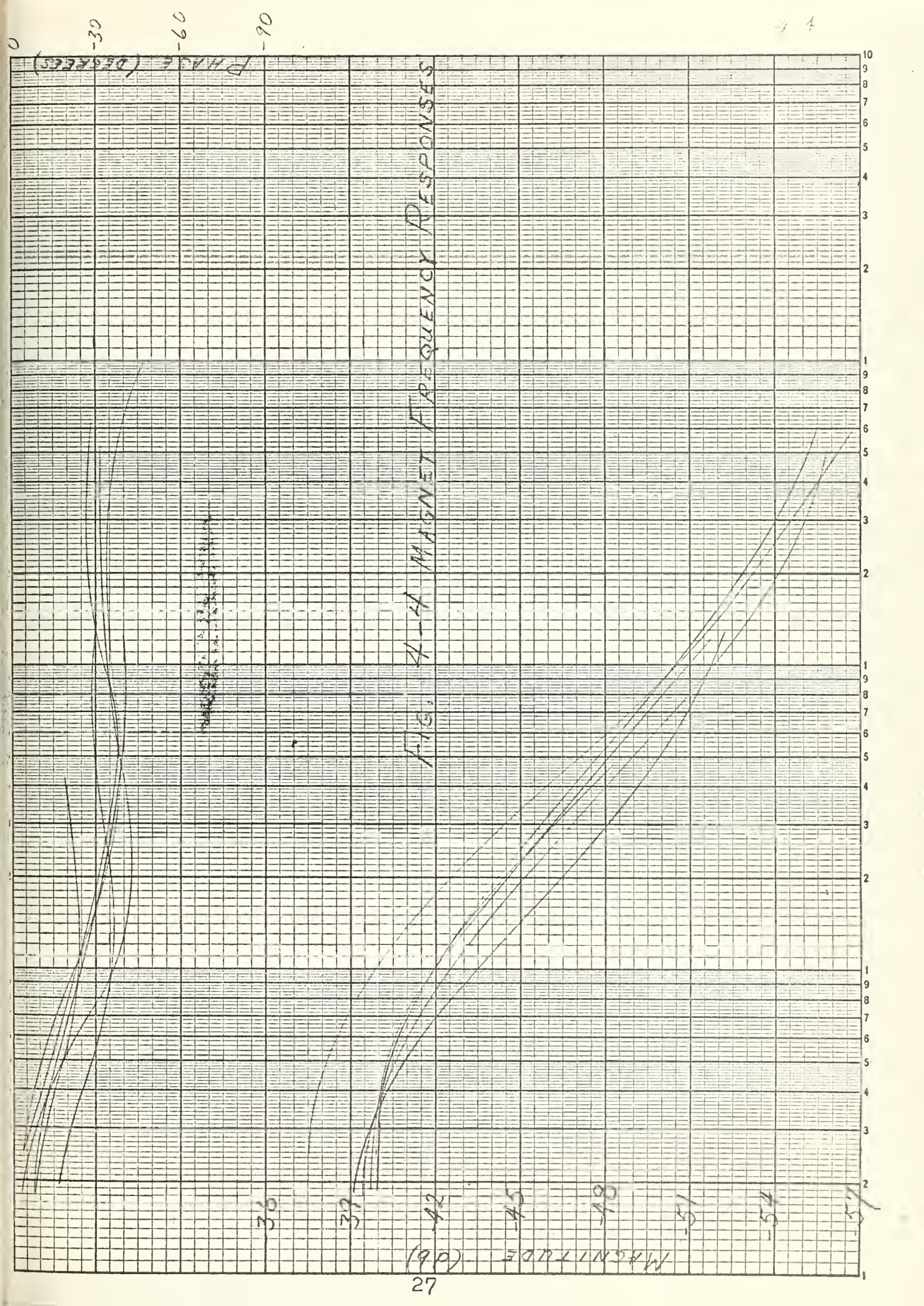


FIG. A-H MAGNET FREQUENCY RESPONSES

0  
9  
8  
7  
6  
5  
4  
3  
2  
1  
0  
Phase (degrees)

0  
1  
2  
3  
4  
5  
6  
7  
8  
9  
10  
MAGNITUDE (dB)

FIG. 4-5  
AVERAGE  
MAGNET FREQUENCY  
RESPONSE

36  
39  
42  
45  
48  
51  
54  
57

-30  
-60  
-90

Phase (degrees)

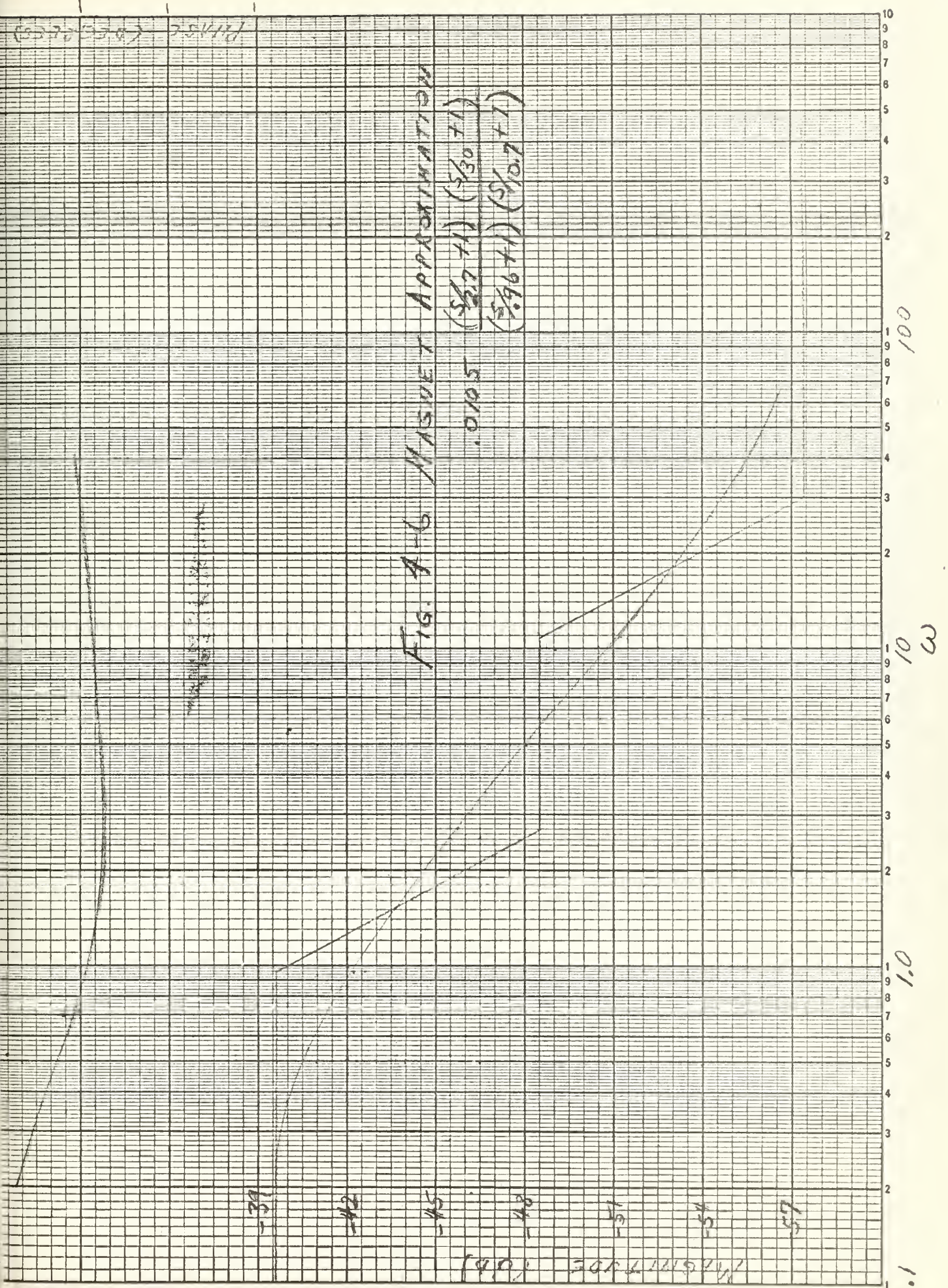


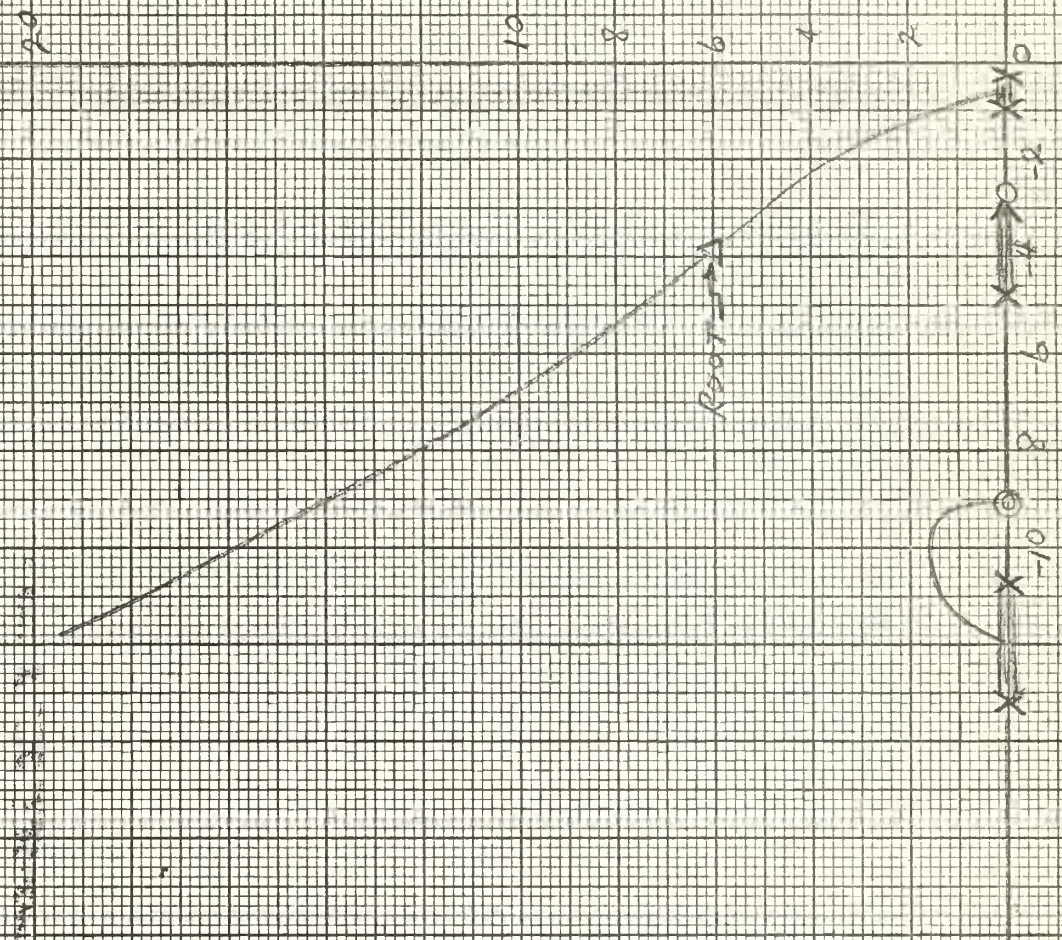
FIG. 4-6 MAGNET APPROXIMATION

-39  
-42  
-45  
-48  
-51  
-54  
-57

Magnitude (dB)

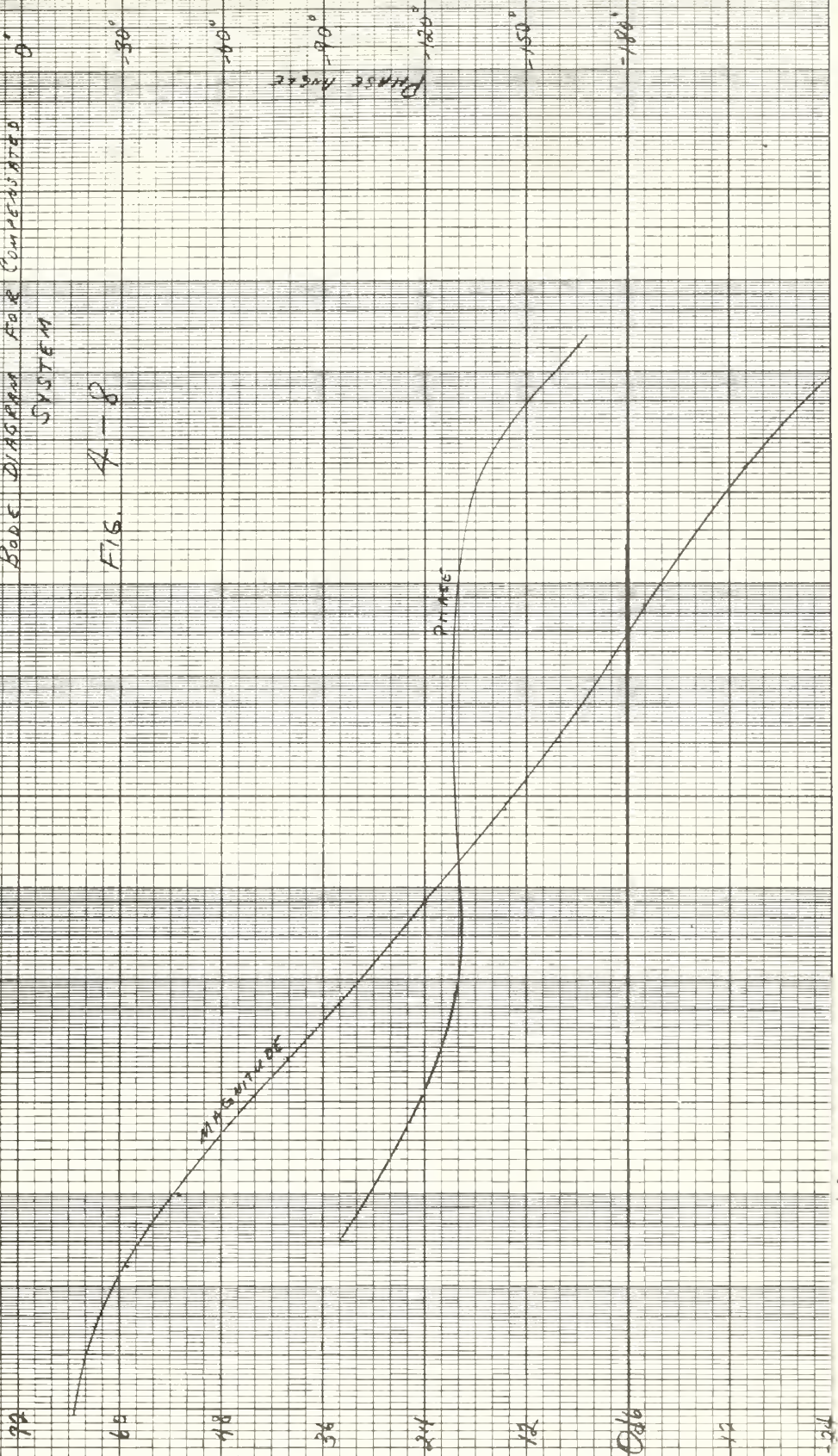
COMPENSATED SYSTEM  
Root locus

FIG. 4-17



BODE DIAGRAM FOR COMPENSATED SYSTEM

FIG. 4-8



from the observation of the equipment in operation, it was found that sufficient gain adjustment was available at the chopper amplifier to offset the attenuation of this extra filter.

## 5. Conclusions

The experimental analysis conducted on the generator and magnet circuit established accurate representations for these two parts of the regulating system. It indicated that the magnet circuit was not significantly amplitude sensitive in the operating range, and a linear approximation was obtained.

Using the new magnet and generator data, analysis still indicated that the system response should be satisfactory.

Any difficulties in operation had to be the result of some factor not accounted for in the block diagram. The magnet and generator were checked experimentally. The minor feedback (compensating) loop response was also verified experimentally and agreed well with the transfer function used, even though an additional parallel tee filter was in the circuit to reduce noise. There was no reason to doubt the validity of the chopper amplifier transfer function.

This left two factors which it was felt could have caused the trouble— noise — or the D.C. amplifier,  $I_2$ , or both.

In the design report, reference one, mention was made of a low frequency ripple (about one cps) in the magnet current, which was attributed to noise from the generator at a frequency of about 59 cps, which mixed with the chopped error signal. The oscillation mentioned on the first page of section four was of this form so that this noise

problem may not have been completely eliminated.

It was found that the D.C. amplifier,  $K_2$ , could not be considered as a fixed gain, 3.64, over the entire operating range, as shown in the block diagram. To keep  $K_2$  constant for all values of reference voltage, it was necessary to make a bias adjustment at  $K_2$ .

Thus, the solution to the problem appears to lie in more effective reduction of noise effects from the generator, and replacement of  $K_2$  by an amplifier which is effective without adjustment, over the entire operating range of reference voltages.

## BIBLIOGRAPHY

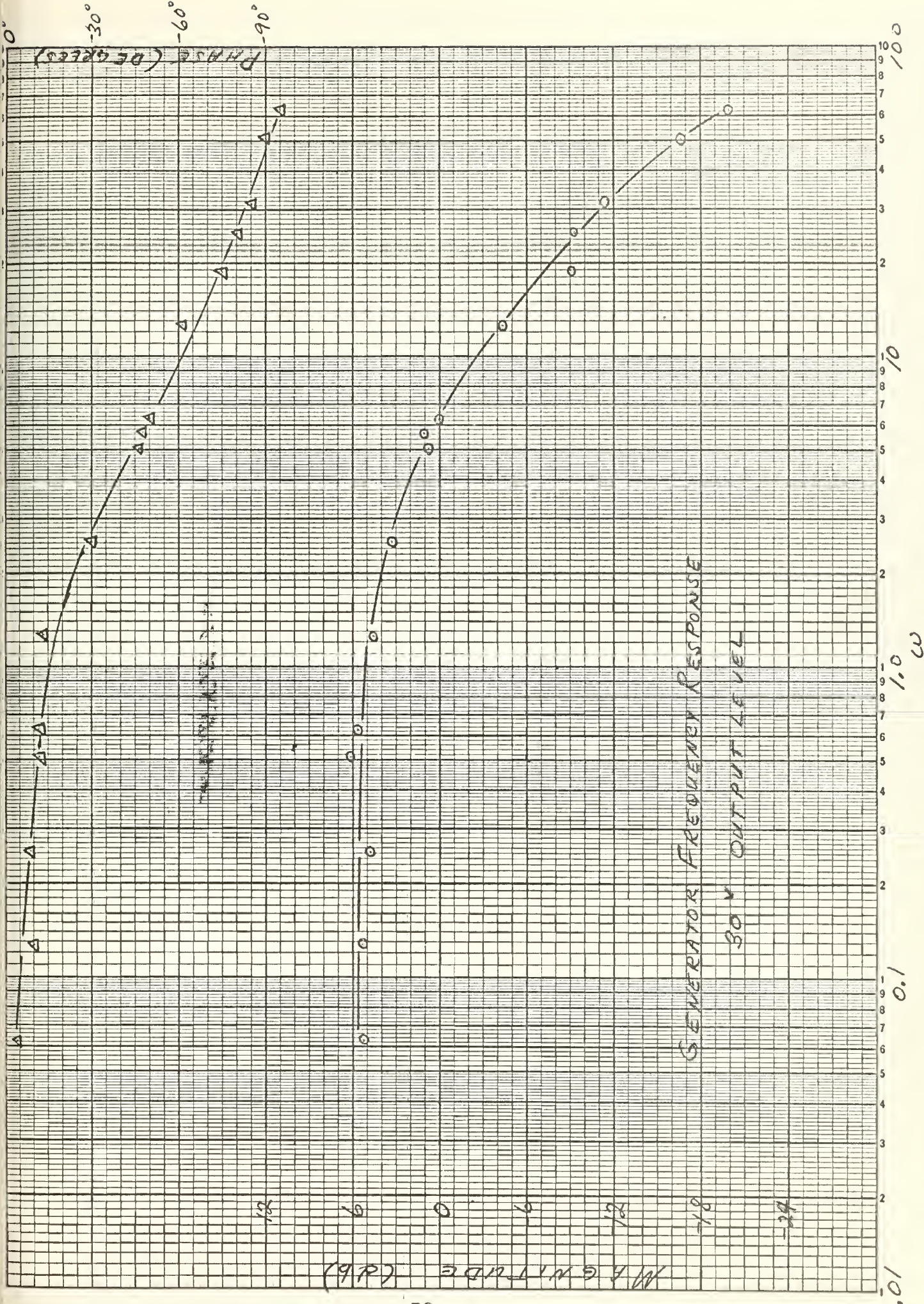
1. Lawrence Radiation Laboratory report LL 275-1 of November 12, 1958, Compensation of a Current Regulated Generator for the 90" Cyclotron Bending Magnets.
2. G. J. Thaler and M. P. Pastel, Analysis and Design of Nonlinear Feedback Control Systems, McGraw-Hill Book Company, Inc., 1962.

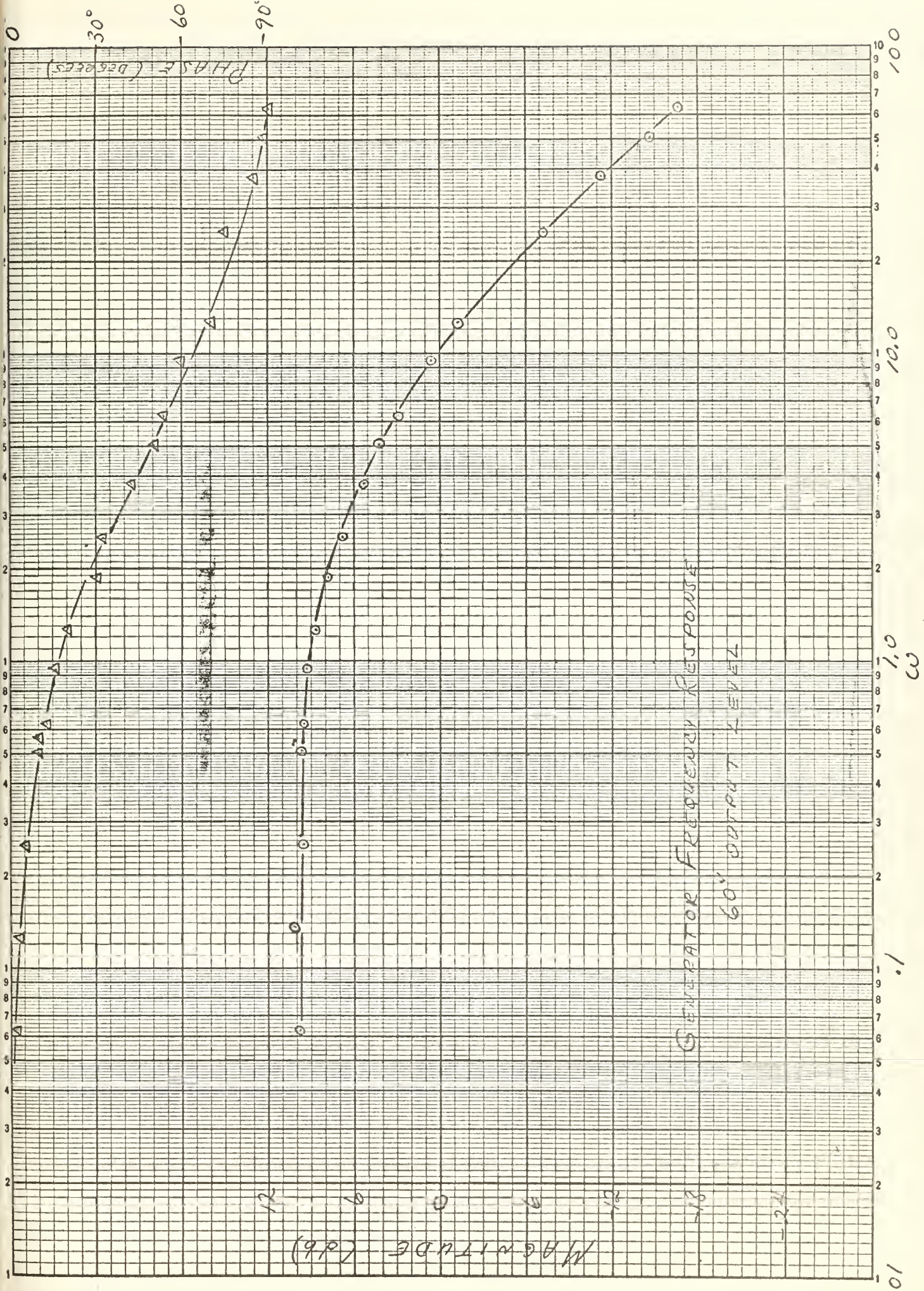
Appendix I

Generator Frequency Responses

The following frequency responses are for the generator at different voltage outputs. The response was nearly the same for all output voltages.

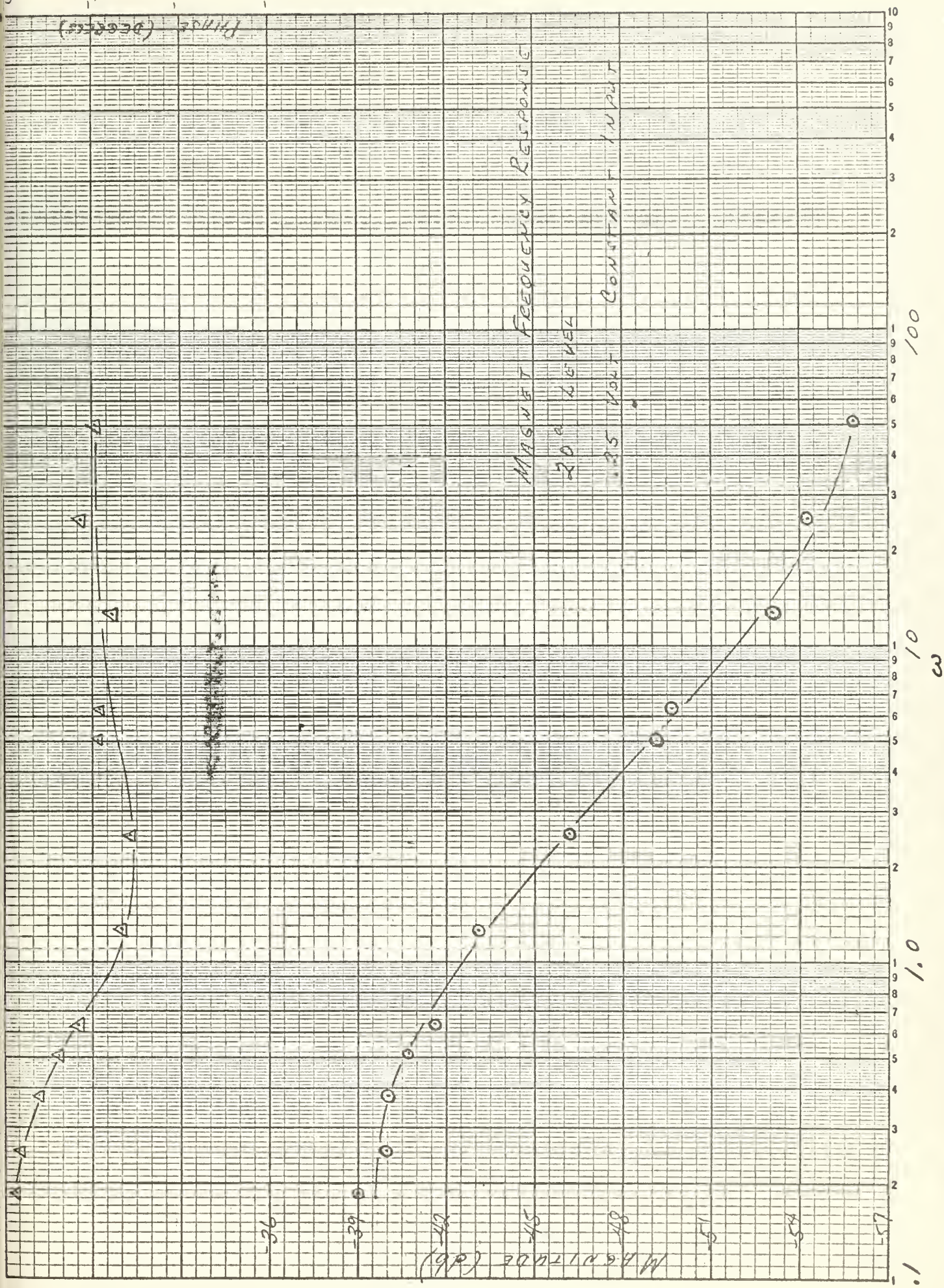
All responses were taken with inputs at the d.c. amplifier,  $K_2$ . The 60 volt curve, page 39, includes a 5.7 db gain due to  $K_2$ . The 30 volt curve, page 38, has been corrected, by subtracting  $K_2$  (db).

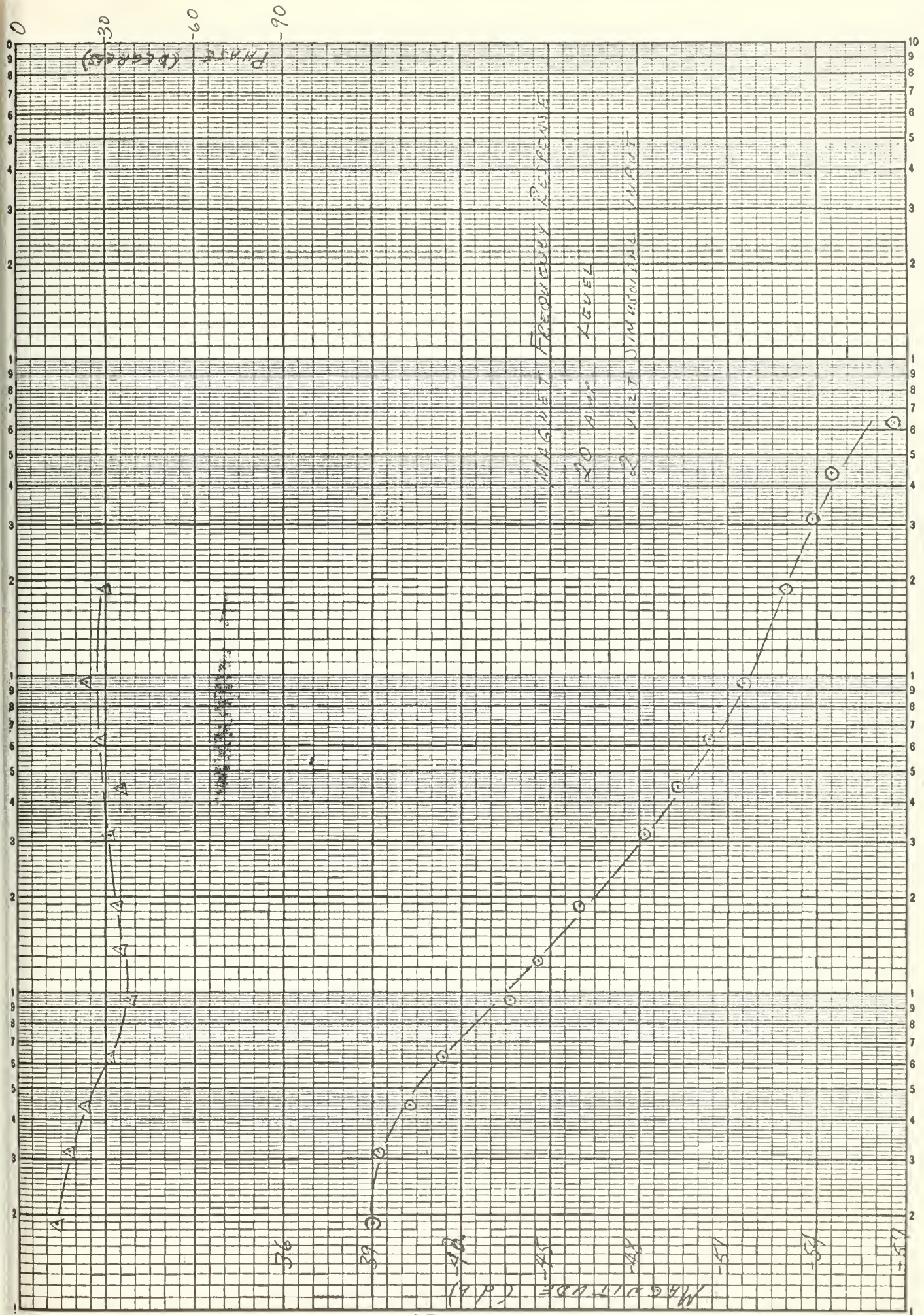


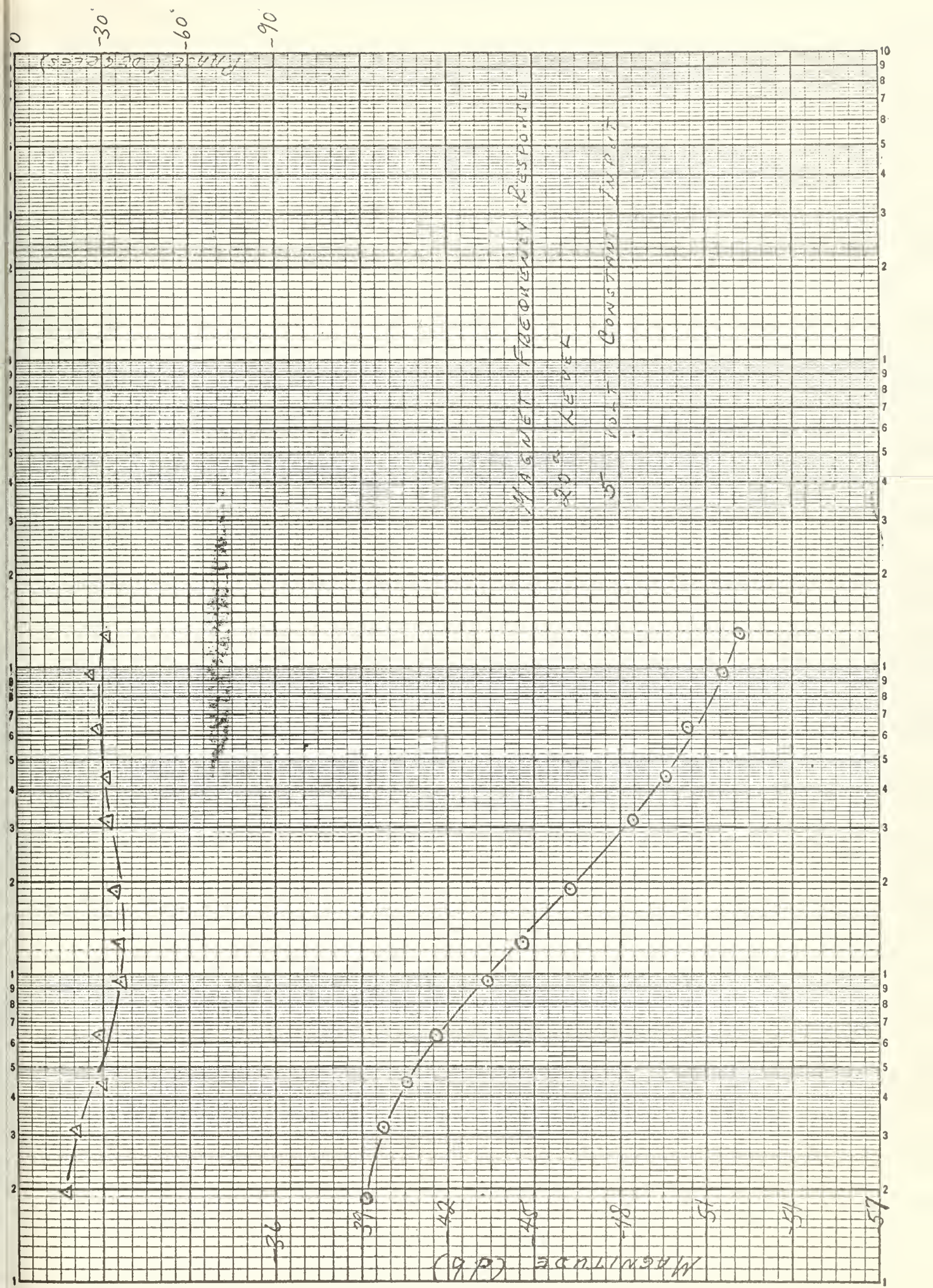


Appendix II  
Magnet Frequency Responses

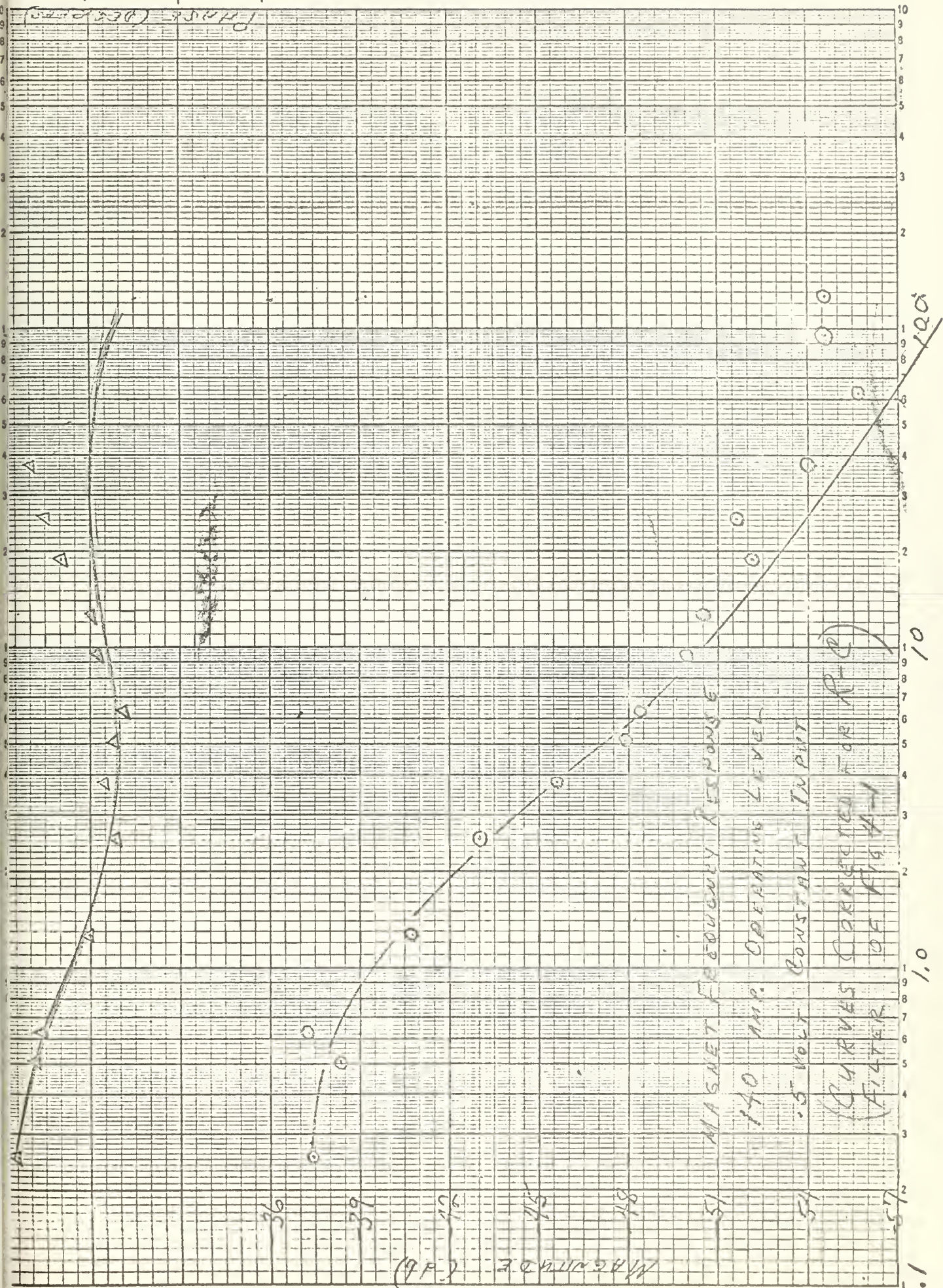
The following curves are some frequency responses for the magnet, at different operating conditions and input amplitudes. These are some of the responses used in the magnet analysis of section four. On each curve is indicated the magnet current level for the response, and the value of constant input in volts, maintained at the input to the magnet throughout the run.

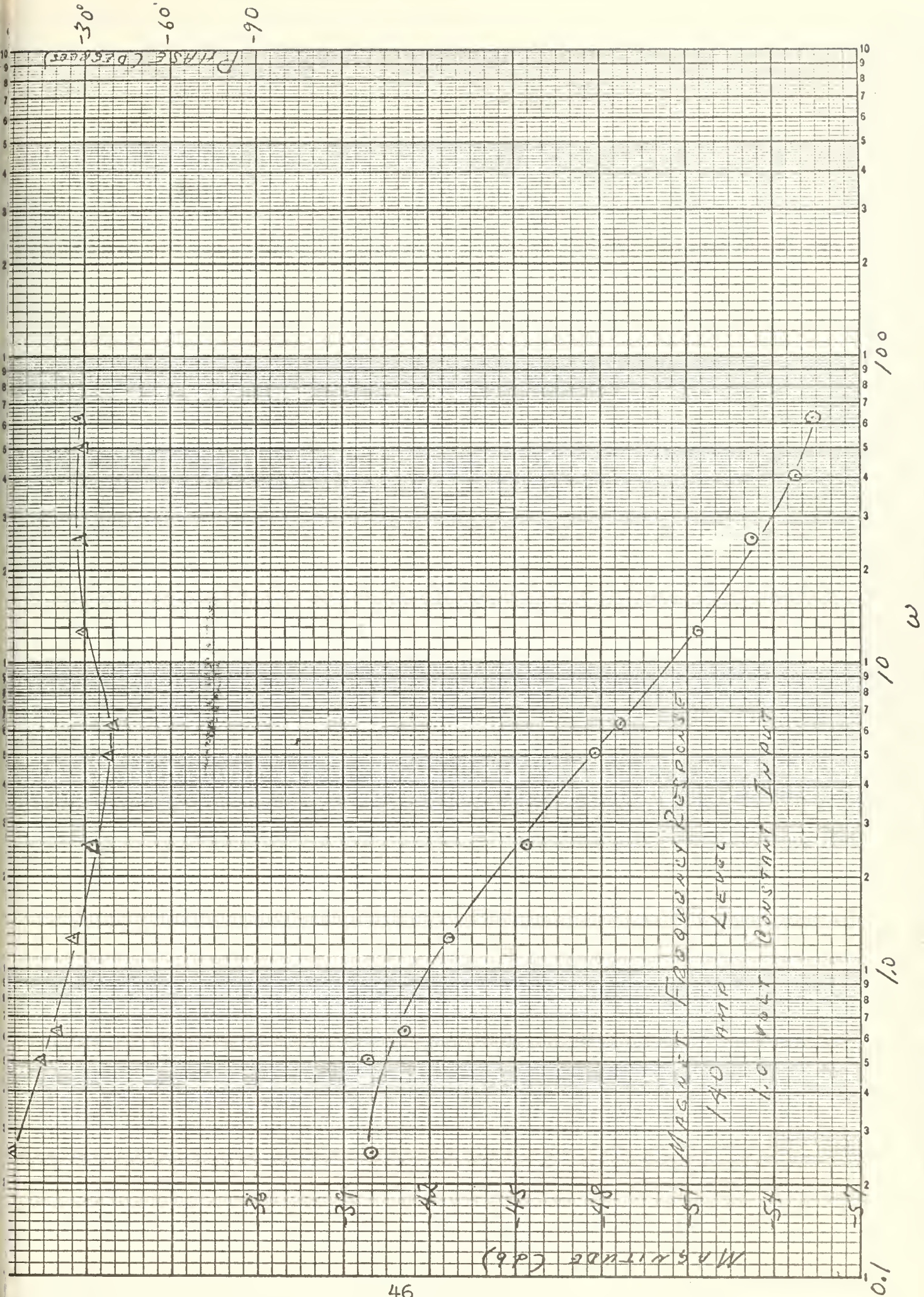






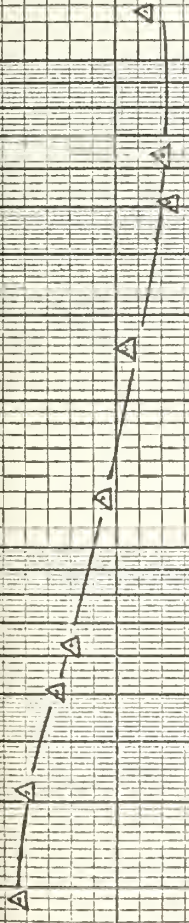
-30°  
-60°  
-90°





-30  
-60  
-90

Phase (Degrees)

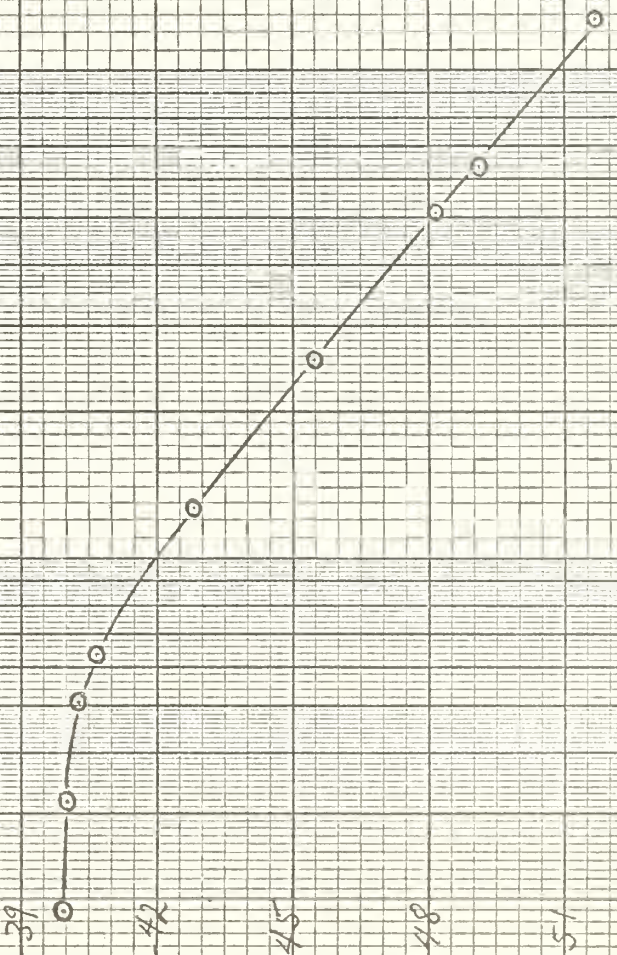


~~Phase Plot~~

MAGNITUDE (dB)

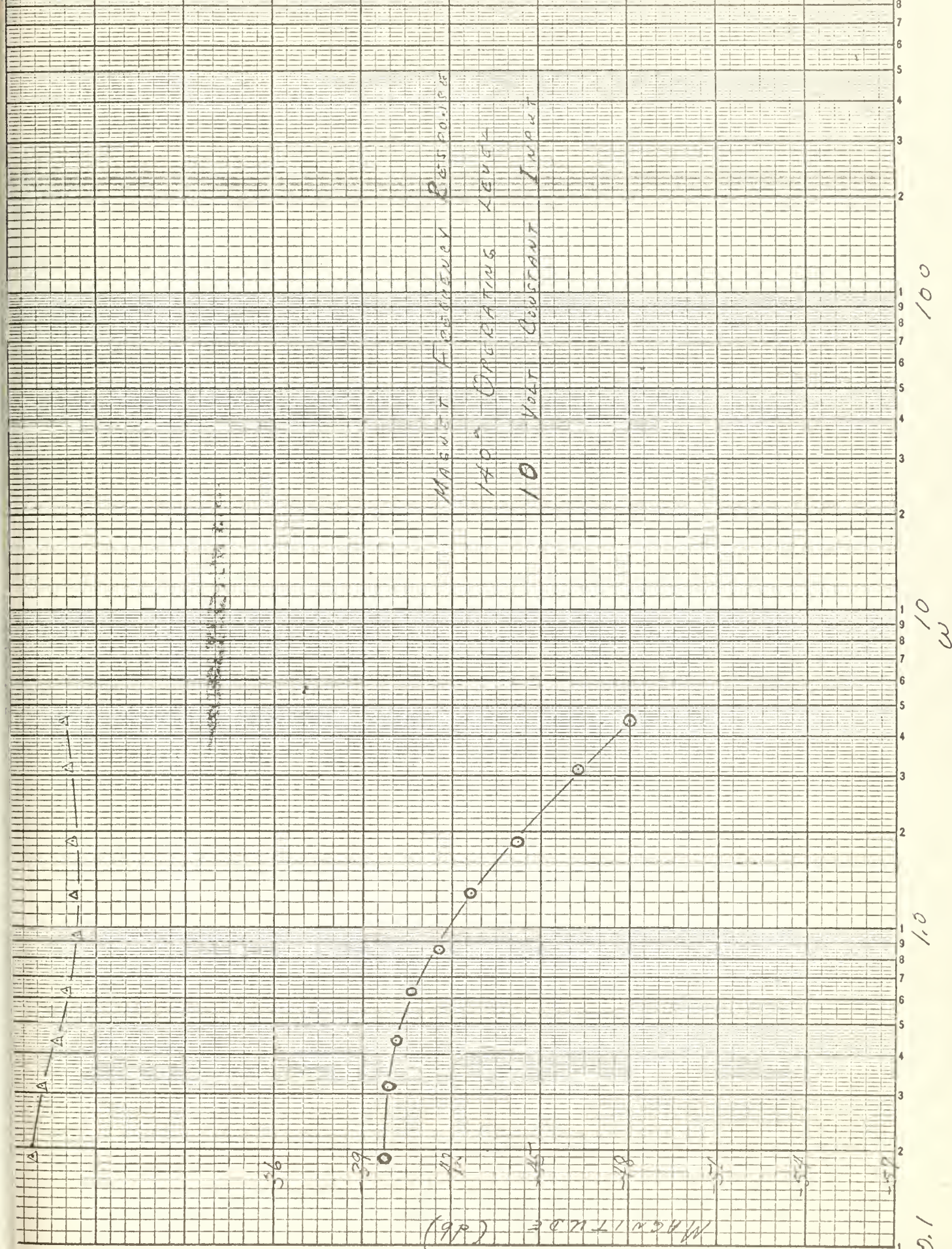
36  
39  
42  
45  
48  
51  
54  
57

MAGNET FREQUENCY RESPONSE  
140<sup>2</sup> OPERATING LEVEL  
3 VOLT CONSTANT INPUT



100  
10  
ω  
1.0  
0.1

PHSR (DEGRASS) -30  
-60  
-90



100  
10  
1.0  
0.1

thesC373

An analysis of a current regulator for a



3 2768 001 02374 0

DUDLEY KNOX LIBRARY